

INTERANNUAL RESPONSE OF VEGETATION TO CLIMATIC VARIABILITY IN A COASTAL SAVANNA IN CALIFORNIA

Monica Garcia and Susan L. Ustin

Center for Spatial Technologies and Remote Sensing (CSTARS)
Department of Land, Air and Water Resources, University of California, Davis, CA 95616

1. INTRODUCTION

Ecosystem responses to interannual weather variability are large and superimposed over any long-term directional climatic responses, making it difficult to assign causal relationships to vegetation change. Better understanding of ecosystem responses to interannual climatic variability is crucial to predicting long-term functioning and stability. Hyperspectral image analysis has the potential to detect ecosystem responses that are undetected by broad band sensors and can be used to scale to coarser resolution global mapping sensors, e.g., MODIS. However, increases in temporal coverage of sites will be necessary to understand vegetation dynamics.

Stanford University's Jasper Ridge Biological Preserve has received more frequent data acquisitions than any other site over the past nine years, permitting an examination of the sensitivity of vegetation response to seasonal and interannual weather conditions detectable by hyperspectral imagery. The purpose of this project is to identify the type and magnitude of short-term responses of vegetation to interannual climatic variations, utilizing remote sensing techniques in a natural savanna located in the Central Coast Range in California. The interpretation of those responses detected with hyperspectral sensors is based on the ecological context.

2. MATERIALS AND STUDY SITE

Jasper Ridge Biological Preserve (JRBP) is located in the eastern foothills of Santa Cruz mountains, at 37° 24' N latitude and longitude 122° 13' 30" W. A vegetation map was produced from aerial photographs and modified based on field observations by N. Chiarello. The 500 ha of JRBP are composed of five main vegetation types: evergreen, deciduous, chaparral, wetlands, and grasslands. Topography and soil patterns create relatively high spatial heterogeneity (<http://jasper1.stanford.edu>; Chiarello, 1989; Ustin et al., 1998).

Two AVIRIS (Airborne Visible Infrared Imaging Spectrometer) images of JRBP were used in this study. They were acquired on 05/03/1996 and 04/29/1998 following northeast and northwest flight lines respectively. They have a nominal ground pixel size of 20 m and spectral resolution of 10 nm. Radiometric resolution is 65536 DN (16 byte data). The choice of images was driven by the great difference in annual rainfall between the two years and the proximity of image dates. The 1995/1996 and 1997/1998 seasons were within a weak "La Niña" and a strong "El Niño" event respectively, which in California are expressed in dry and wet years. In the 1995/1996 season, total rainfall was 794 mm and in the 1997/1998 season it was 1333 mm.

A Digital Orthophoto Quad (DOQ) from USGS corresponding to Palo Alto South West (PASW) quadrangle in UTM coordinate with 1 m pixel resolution was used to georeference the 1998 scene using 43 points. The RMSE using a first order polynomial warp was less than 0.05 pixels or 1 m. The study area of 500 ha is without large topographic gradients therefore, adjusting a polynomial function works well. The 1996 image was georegistered to 1998 image, to ensure that change detection was accurate, using 44 points. The error was less than 0.4 pixels or 8 m, also using a first order degree polynomial.

Apparent reflectance was calculated in both images using a modified MODTRAN model (Green, 1991). Later, they were radiometrically aligned to an April 1997 image of Jasper Ridge by regression to Pseudo Invariant Features (PIF). The 1997 image was provided by Dar Roberts and had been aligned with field spectra obtained that year. It is remarkable that signal to noise (S/N) levels improved in 1998 by almost a factor of two in most spectral regions. Thus in 1998 the highest S/N levels calculated for a 50 % reflectance target at the sea level and 23.5° zenith angle corresponds to the A spectrometer (0.7 μm) with levels of 1000:1, and the lowest were measured in the De spectrometer in the SWIR region (2.2 μm) with maximum levels of 400:1 (Green et al., 1999).

3. METHODS

In change detection studies, sources of variation in reflectance between dates other than surface changes must be minimized (Yuan et al., 1998; Lunetta, 1998). Repeatability from 1996 to 1998 was ensured through atmospheric calibration and radiometric image alignment. Illumination and phenological differences were minimized as dates of image acquisition in both years were only one week apart. Comparison with NDVI biweekly composites from AVHRR temporal series between 1996 and 1998 in the area of study shows that mean trends in NDVI are at the peak of their greenness on both dates (unpublished data).

The method used to detect and quantify changes between years was linear spectral unmixing (Adams et al., 1986). There are several advantages of using linear unmixing instead of vegetation indices or other classification methods to study landscape structure and dynamics, especially in semi-arid areas, where cover is low and then soil and litter greatly affect pixel reflectance (Asner, 1998; Elmore et al., 2000; Roberts et al., 1993; Smith et al., 1990; Ustin et al., 1993, 1998). In fact, linear spectral unmixing has been widely used both with hyperspectral and TM data at Jasper Ridge and other semiarid areas with even lower primary productivity. (Elmore et al., 2000; Ustin et al., 1993, 1998; Smith et al., 1990). In this project, fractions were constrained to sum up to one, but not to be greater than zero as that would eliminate information about the appropriateness of the endmembers (Ustin et al., 1998).

A critical step for the unmixing process was to find spectrally pure endmembers. Image endmembers match the conditions of the vegetation more closely than library reference endmembers, especially in Mediterranean climates where phenological differences account for great changes in biomass between dates. A hybrid method combining automatic and supervised endmember selections was performed on the 1998 image. The methodology proposed by Boardman et al. (1995) to obtain automatic image endmembers was followed. After removing water vapor and noisy bands, to reduce data dimensionality and remove noise, the Minimum Noise Fraction (MNF) algorithm was applied to the reflectance image. Later, Pixel Purity Index (PPI) was calculated in regions of interest at Jasper Ridge, selected following decreasing variance within this new dimensional space. The pixels with the highest PPI values were selected, as they are linearly independent in most dimensions. The same process was performed in the 1996 image in order to be sure that the results are similar. Endmembers used in the unmixing process come from the 1998 image as vegetation was greener and because signal-to-noise levels were improved with respect to 1996.

Root Mean Square Error (RMSE) limited to the Jasper Ridge area was used as a criteria for endmember selection as it gives a general idea about goodness of fit of unmixing. RMSE is defined for each pixel as follows:

$$RMSE = \sqrt{\sum_{\lambda=1}^n (R_o(\lambda) - R_u(\lambda))^2}$$

where $R_o(\lambda)$ is the apparent pixel reflectance, $R_u(\lambda)$ is modeled pixel spectral reflectance and n is the number of bands.

An analysis of the specific contribution from each spectral band to final error and spatial variation in the error can aid in explaining weaknesses in the model. Thus, residuals between observed and modeled reflectance were calculated per band and per pixel. The RMSE were used to assess unmixing results and improve them in areas where adjustment was poor. Although goodness of fit is considered when residuals are at the level of instrument noise (Smith et al., 1990), there are additional error sources derived from the spectral and radiometric calibration procedure, in-flight system changes, solar irradiance model errors, and inaccuracy in parameter estimation (Boardman et al., 1998). In our case, the threshold level chosen for the goodness of fit in the model was 3 % of maximum apparent reflectance in each band. As error is correlated with reflectance levels, the maximum error was restricted to Jasper Ridge.

Interpretation of the causes of high residuals is not always easy without field data. A combination of factors decreases the fitness of the model. One group includes those spectral features not accounted for by the endmembers. Thus, biochemical and structural characteristics of components not included in the model, like litter, or gradual changes in spectral properties due to natural heterogeneity in soil and vegetation at leaf and canopy levels across the scene will contribute to this error. Another source of error, due to the model itself is caused by non-linear mixing effects associated with multiple scattering of photons, especially in the NIR and SWIR bands. Vegetation structure and leaf optical properties, or high reflectance from background cause non-linear scattering effects. Finally,

systematic errors due to illumination and atmospheric conditions, sensor effects, and calibration procedures increase error levels in the model (Asner, 1998; Roberts et al., 1993; Ustin et al., 1998).

Effects of non-linear spectral unmixing are evident in the NIR range as leaf absorption is very low at those wavelengths. The degree of non linearity caused by multiple scattering of photons depends on leaf transmittance, which is lower in xerophytic vegetation like chaparral or evergreen and higher in some grasses and deciduous trees (Roberts et al., 1993; Ustin et al., 1993, 1998). Non-linear mixing also increases with canopy cover and with background reflectance due to brighter soils and standing litter (Asner, 1998; Otterman et al., 1995; Huete et al., 1987; Roberts et al., 1993).

4. RESULTS AND DISCUSSION

Endmember selection

Automatic endmembers selected initially included different vegetation types, dry grass, and soils. Although selection was made in MNF space, endmember separation was related to physical differences affecting spectral properties. Pixels with the highest PPI in MNF space corresponded to soil, vegetation and water spectra. However, Jasper Ridge has a high degree of patchiness because spring grasses grow almost everywhere, and no pure soil pixels could be found. A soil from a bare field east of JRBP was used after evaluating different soil spectra and unmixing results. The water endmember from a lake outside Jasper Ridge was selected as the shade component, because its albedo was the lowest in the entire scene. (Figure 1)

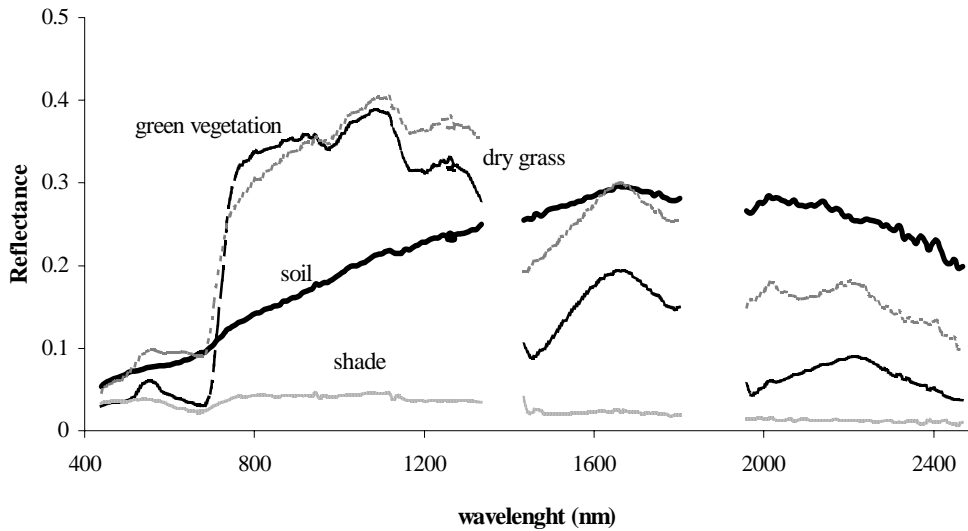


Figure 1. Set of endmembers used for unmixing. Green vegetation and dry grass were selected automatically based on PPI, soil by visual inspection and shade by minimum albedo levels in the image corresponding to a lake.

Linear spectral unmixing was performed applying several different combinations and numbers of endmembers. Final selection relied upon realistic fraction distributions and RMSE levels. The best general fit for the Jasper Ridge area corresponds to a combination of vegetation from evergreens, soil and shade spectra. Adding an additional endmember litter did not improve the general fit, as at this time of the year, all vegetation types but grass are green with little canopy litter, and because the litter endmember was confounded with soil. Figure 2, shows an RGB composite of soil, green vegetation, and shade fractions.

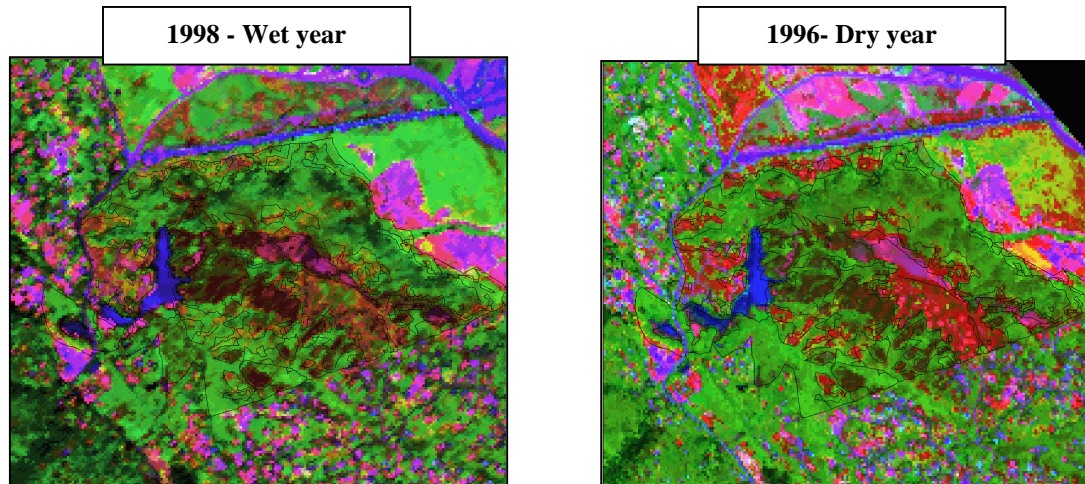


Figure 2: Unmixing using three endmembers: soil (red), green vegetation (green) and shade (blue) in spring at Jasper Ridge.

Error analysis

Mean RMSE in Jasper Ridge area when unmixed with three endmembers were 0.84 % in 1996 and 0.64 % in 1998, with standard deviations of 0.43 % and 0.21 %. Lower error levels in 1998 compared with 1996 can be related with improvements in the A and D spectrometer in 1998. However, spatial distribution of RMSE, shows speckled areas with high RMSE in the grasslands that began to senesce. In addition, green cover is lower and soil background effects are higher than other vegetation types.

Per band residuals between observed and predicted reflectance analyzed over the entire image were in the worse case below 4 % reflectance (Figure 3). However, the spatial and spectral analysis of residuals shows that the error contribution of each band is different and varies depending on vegetation type. It also highlights spectral differences between years. Figure 3 shows that almost all vegetation types fit within error threshold levels except the grasses. Both serpentine and greenstone grasses had high residuals in the red, NIR and SWIR bands in 1996 and 1998. When residuals are high and positive in the visible range, the model overestimates vegetation or underestimates soil, as vegetation reflectance is very low in this range. In the same way high negative residuals in the NIR reflect an overestimation of vegetation as observed reflectance is lower than modeled and vegetation reflectance dominates in the NIR wavelengths.

These errors can be related to decreases in chlorophyll absorption (high positive residuals in the red) and leaf water content (in the SWIR) and high negative residuals in the NIR, which respond to lower than predicted NIR-plateau reflectance. As a consequence the red-edge is shifted towards the blue region, decreasing the fitness of the green endmember. All these characteristics are associated with senescent grasses and plant litter. This effect is stronger in 1996 than in 1998 corresponding to a more xeric situation. The error attributable to extrapolation of endmembers from 1996 to 1998 does not account for changes as residuals in other vegetation types, such as evergreen forest and chaparral, are of the same order in both years. In 1996, high negative residuals in SWIR bands may be responding to increased cellulose and lignin absorption.

The effect of greater scattering with greater canopy cover is shown in Figure 4 for deciduous forest pixels that have high leaf transmittance. There, soil fractions in general are low and adjustments come from vegetation and shade fractions. The observed spectra had the same spectral features but different albedo, which is related to greater canopy cover.

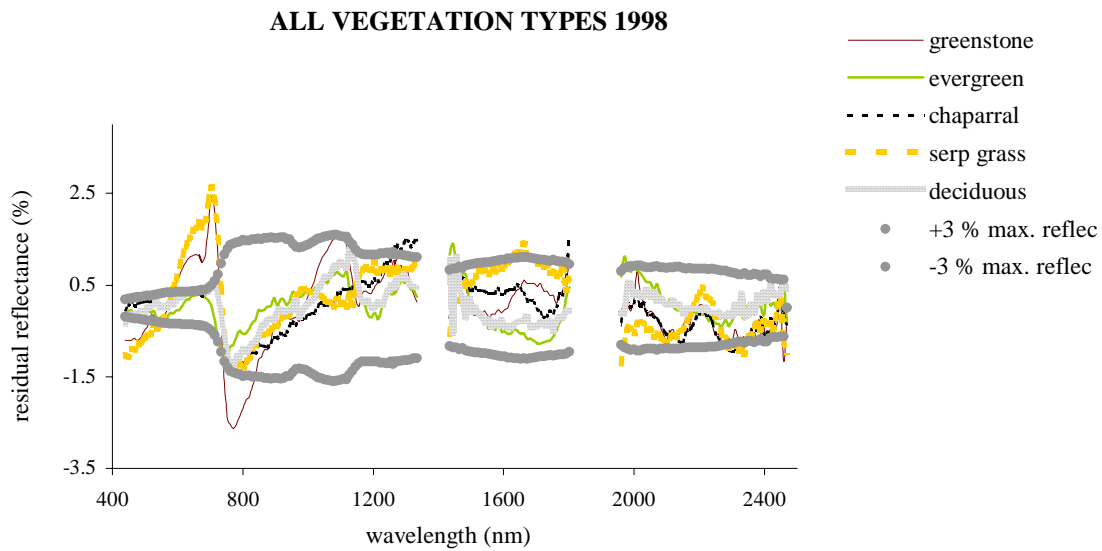
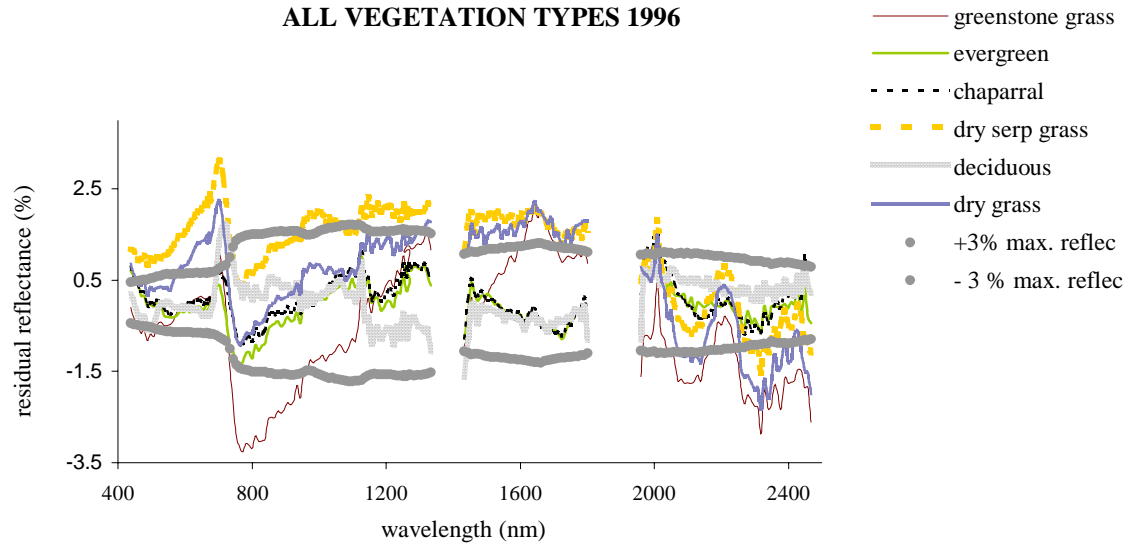


Figure 3. Comparison of residuals across spectral bands between observed AVIRIS reflectance and modeled with unmixing in 1996 and 1998 for different vegetation types. Grasses present higher residuals as a consequence of senescence.

In Figure 4, residuals are plotted for grasses with different backgrounds: serpentine and greenstone soils. When green cover is high, reflectance residuals are low. However, with lower canopy cover, spikes in the red edge are high for greenstone and serpentine grasses, suggesting non-modeled reflectance from either litter or soil. In the NIR, negative residuals indicate overestimation of vegetation. At this time of the year, serpentine grasses are drier than greenstone grasses, which explains the lower negative residual in the NIR. However, in the red-edge, residuals are greater for greenstone grasses, where the soil is brighter, which increase non-linear scattering more than darker serpentine soils. This suggests that the effect of litter is strongest in the NIR and the effect of soil is more important near the red-edge.

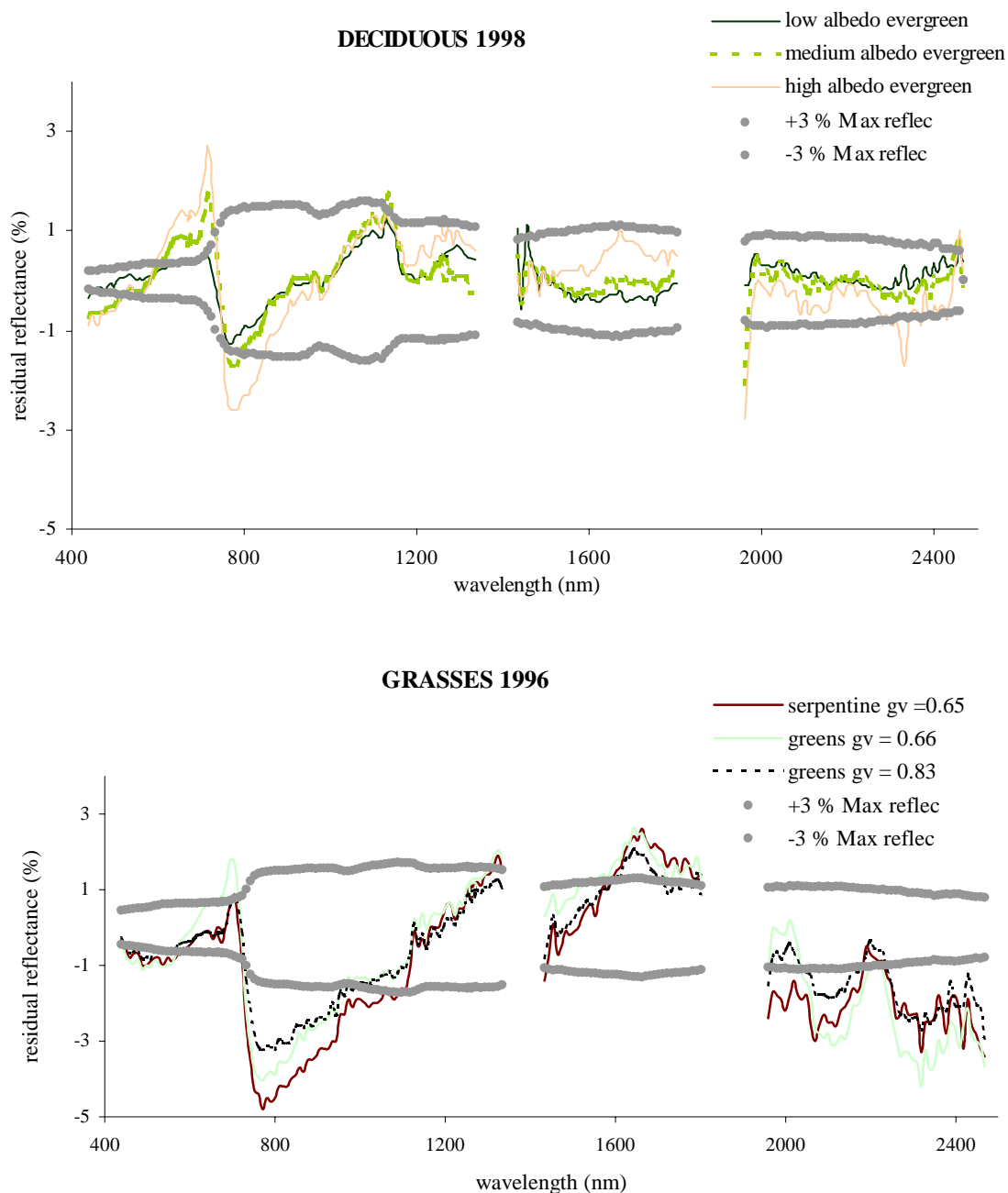


Figure 4: Residuals between observed and predicted reflectance suggesting non-linear scattering effects due to increasing canopy levels in high transmitting foliage and background effects from soil and litter in the grasses.

Standing litter increases reflectance at 680 nm, reduces NIR reflectance, increases the slope of NIR between 800 and 1000 nm, and increase SWIR reflectance similarly to stems in trees and shrubs (Asner, 1998; Otterman et al., 1995). However, small increases in standing litter cause more than proportional increases in canopy reflectance because of non-linear mixing especially in NIR and SWIR regions (Asner, 1998). Figure 5 shows residual trends for chaparral canopies and serpentine and greenstone grasses are similar, but the magnitude is greater in grasses despite similar cover fractions. Also, serpentine grasses present the red-edge shifted with respect to greenstone grasses due to greater decreases in chlorophyll absorption, as they senesce earlier than greenstone grasses.

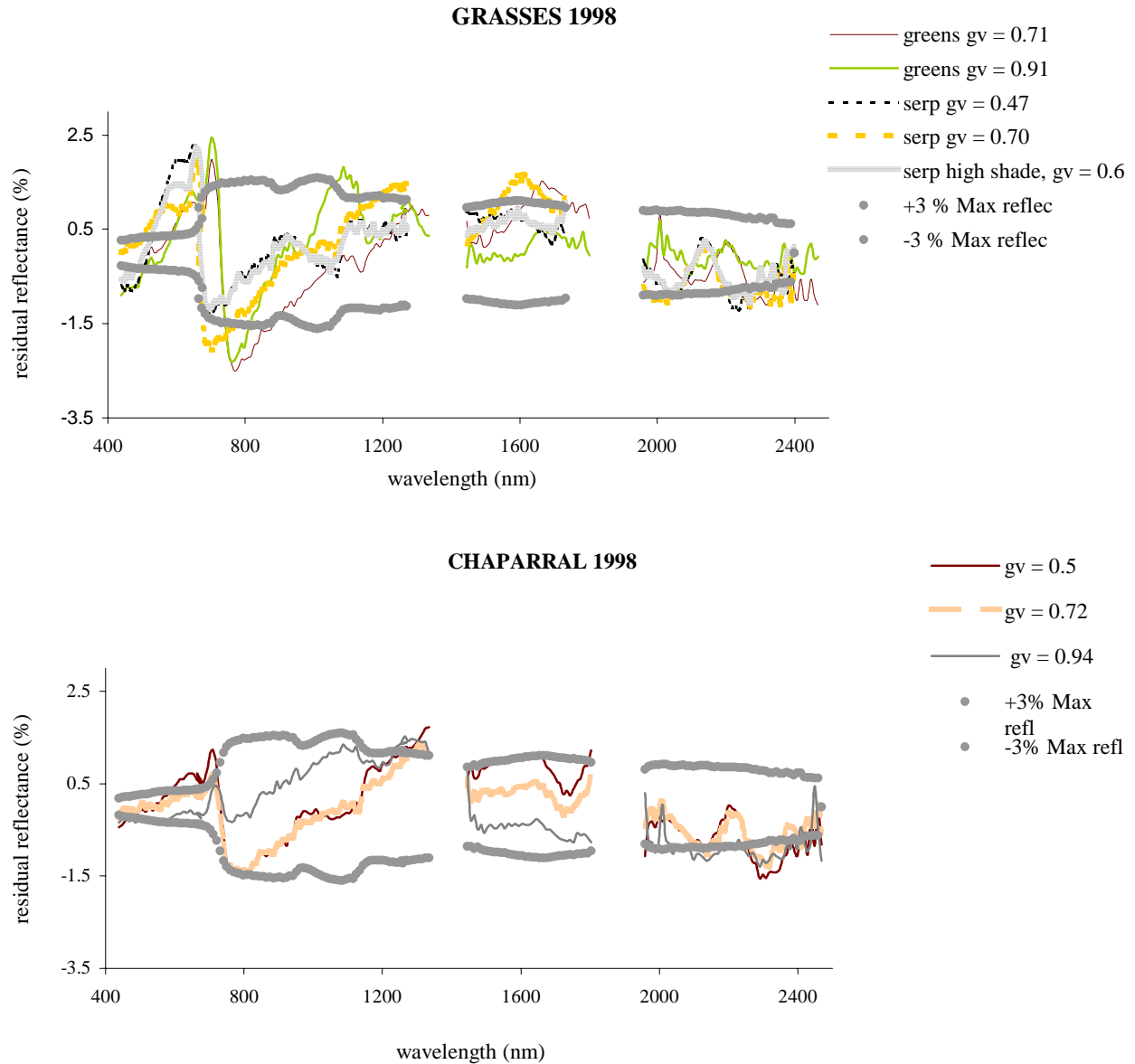


Figure 5. Differences in residuals between grasslands and chaparral areas showing non-modeled reflectance from dry grass and litter at the red-edge and in the SWIR regions.

Unmixing with four endmembers in grassland areas

Non-linear unmixing effects can lead to over estimation of green vegetation fractions making change detection results unreliable. For this reason and based on the previous analysis, an additional endmember was added in the grassland areas to account for the unexplained reflectance. A senescing but not totally dry greenstone grass was chosen as the fourth endmember based on the PPI ranking (Figure 1). Unmixed fractions were consistent with the phenological stage of the grasslands at the end of April and error levels decreased, being on the same order as the mean RMSE using three endmembers for the other vegetation types. Trials using a drier litter endmember, without red-edge, yielded negative and unrealistic fractions with high RMSE.

In conclusion, the final unmixing results consisted of soil, evergreen and shade fractions for Jasper Ridge except in serpentine and greenstone grass where additional endmember of dry grass was included. Grassland

boundaries were delimited using Jasper Ridge vegetation map. Soil and vegetation fractions were rescaled to sum to 100 after removing the shade fraction. It was assumed that shade fractions are equally distributed between soil and vegetation components. However, if shade fractions are contributed by shadows and not by photometric shade, subpixel topography can affect materials differently and rescaling fractions will be inaccurate (Smith et al., 1990). Comparison of shade fractions against a DEM did not reveal a vegetation dependent residual shade.

Differences in mean unmixed fractions

Mean fractions of green vegetation (gv), soil and nonphotosynthetic vegetation (npv) or dry grass were calculated both years and each vegetation polygon (Figure 6). Herbaceous annuals are most affected by increased rainfall in the wet year while chaparral, deciduous, and evergreen forests present less plasticity in their growth response to rainfall. Dry grass fractions were lower in the wet year than in the dry year. However, the sum of green and dry vegetation in both years remained constant. This could reflect changes in phenology more than in primary productivity. Phenological changes in grasslands arise mainly through changes in species composition (Chiarello, 1989), suggesting changes in species composition between dry and wet years.

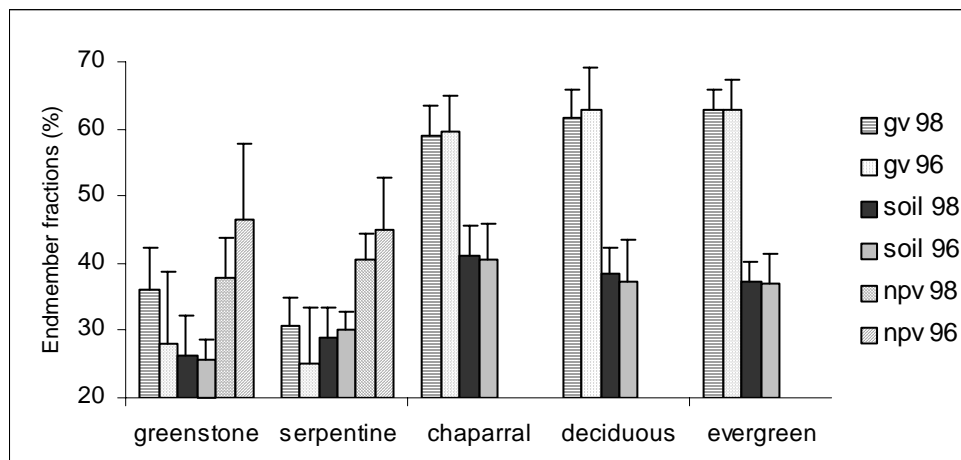


Figure 6. Differences between mean unmixed fractions in 1996 and 1998 calculated for each vegetation community. Error bars represent one standard deviation for the fraction distribution within each vegetation polygon and year.

In any case, the high spatial variability of fractions in a given year makes mean differences insignificant as shown in Figure 6. Differences in structure and geometry among vegetation types can produce different green vegetation fractions for the same biomass limiting comparisons between vegetation types (Gamon et al., 1993)

Change detection using unmixed fractions

One goal of the study was to evaluate interannual changes in relation to spatial variability. Thus, percentage change between 1996 and 1998 was calculated to normalize fractions for all vegetation types. A threshold of one standard deviation was set to determine significant changes, which are mapped in Figure 7. Increases means higher fractions in 1996 compared to 1998.

In general, significant changes in communities (other than grasses) are from increases in green vegetation fractions corresponding to decreases in soil fractions and vice versa. Evergreen communities did not show any changes between years. In some areas of the deciduous forest green vegetation fractions decreased and soil increased in the wet year. One explanation might be due to delays in phenological cycle leading to later peaks in biomass (Chiarello, 1989). Chaparral vegetation shows the greatest change after grassland areas, with both increases and decreases, which may be responding to grass abundance in the shrubland areas.

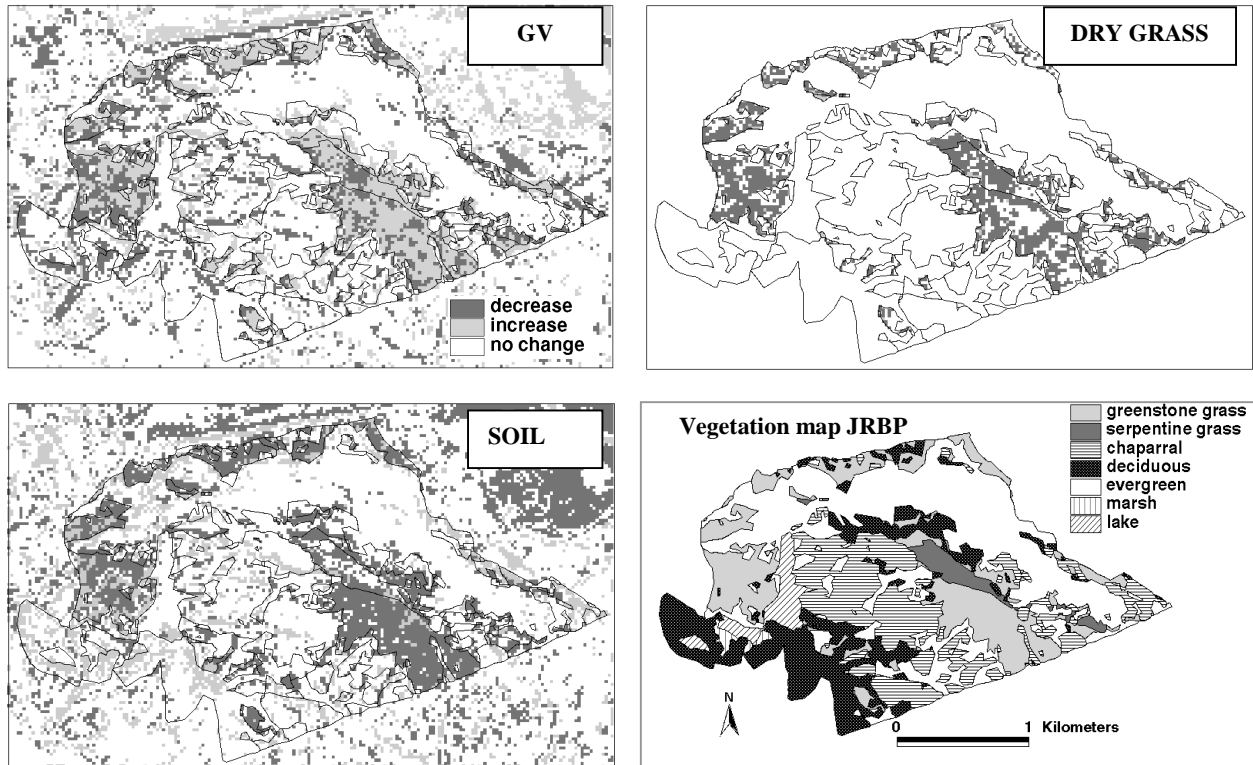


Figure 7. Significant changes in green vegetation (GV), dry grass and soil fractions between 1996 and 1998. Black areas correspond to decreases and gray areas to increases in the wet year (1998) relative to the dry year (1996).

Grasslands show significant changes in green vegetation and soil fractions. The patterns are complex and spatial trends are not always correlated. Thus, in the wet year green vegetation fractions increase in most areas but decreases are also considerable. Soil fractions mainly decreased. The fact that soil fractions can remain constant while green vegetation (GV) can increase indicates that the mixing algorithm can quantify increases in biomass in mixed pixels. However, dry grass fractions in the wet year never increased and either decreased or remain unchanged. When non-photosynthetic vegetation (NPV) decreases, soil fractions, in general, tend to decrease too and green vegetation fractions increase.

5. CONCLUSION

Spectral linear unmixing of AVIRIS data is appropriate to capture some of the complexity of ecosystem interrelations and landscape spatial heterogeneity in a semiarid grassland. Subtle changes in vegetation structure between dry and wet years can be detected. As pixel heterogeneity within a vegetation type is very high, mean differences between years for a vegetation type are not significantly different. However on a pixel basis, significant differences in fractional abundances are detected.

From among all vegetation communities, grasses are the most plastic in response to climatic variability, and spectral changes might be responding to changes in grassland structure as well as abundance. Evergreen and deciduous forests are not as responsive to differences in interannual rainfall as they have access to water layers at deeper soil depths, and both LAI and growth plasticity are less than observed for grasses. In chaparral communities, most of the observed changes are explained by annual grasses growing within the shrub communities.

Improvements in the performance of the AVIRIS instrument explain only partially the better fitness of the unmixing model in 1998 with respect to 1996. In general, non-linear scattering due to senescing vegetation, high green cover or high transmitting foliage also affect the results which can be improved with a different endmember selection in some areas. It would be good to validate these results with field data, and relate vegetation changes to

water and energy budgets. Also, increases in the temporal coverage of AVIRIS would enable following the phenology of the different vegetation communities providing better understanding of vegetation dynamics.

6. REFERENCES

- Adams, J.B., Smith, M.O., and P.E. Johnson, 1986, "Spectral mixture modeling: A new analysis of rock and soil types at the Viking Lander 1 site". *J. Geophys. Res.* 91: 8098-8112.
- Asner, G.P., 1998, "Biophysical and biochemical sources of variability in canopy reflectance," *Remote Sens. Environ.* 64:234-253.
- Boardman, J.W., 1998, "Post-ATREM polishing of AVIRIS apparent reflectance data using EFFORT: a lesson in accuracy versus precision". *Summaries of the Seventh JPL Airborne Earth Science Workshop*. JPL Pub. 97-21, Vol.1, pp 21.
- Boardman, J.W., F.A. Kruse, and R.O. Green, 1995, "Mapping target signatures via partial unmixing of AVIRIS data," *Summaries of the Fifth JPL Airborne Earth Science Workshop*. JPL Pub. 95-1, Vol.1. pp 23-26.
- Boardman, J.W., 1993, "Automating spectral unmixing of AVIRIS data using convex geometry concepts," *Summaries of the Fourth Annual JPL Airborne Geoscience Workshop*. JPL Pub. 93-26, Vol.1. pp 11-14.
- Chiarello, N.R., 1989, "Phenology of California grasslands". In *Grassland structure and function. California annual grassland*, L.F. Huenneke and H.A. Mooney, Eds, Kluwer Academic publishers, pp 47- 56.
- Elmore J.E., Mustard, J.F., Manning, S.J. and Lobell, D.B., 2000, "Quantifying vegetation change in semi-arid environments: precision and accuracy of spectral mixture analysis and the Normalized Difference Vegetation Index," *Remote Sens. Environ.*, in press.
- Gamon, J.A., Field, C.B., Roberts, D.A., Ustin, S.L., and R. Valentini, 1993, "Functional patterns in an annual grassland during and AVIRIS overflight," *Remote Sens. Environ.* 44: 239-253.
- Green, R.O., B. Pavri, J. Faust, and O. Williams, 1999, "AVIRIS radiometric laboratory calibration, inflight validation and a focused sensitivity analysis in 1998," *Summaries of the Eight JPL Airborne Earth Science Workshop*. JPL Pub. 99-17, pp. 161-175.
- Green, R.O., J.E., Conel, J.S. Margolis, C.J. Bruegge, and G.L. Hoover, 1999, "An inversion algorithm for retrieval of atmospheric and leaf water absorption from AVIRIS radiance with compensation for atmospheric scattering," *Proceedings 3rd Annual JPL Airborne Geoscience Workshop*, Robert O. Green, Ed., Jet Propulsion Laboratory, Pasadena, CA, May 20-21, JPL 92-14, pp. 51-61.
- Huete, A.R., 1987, "Suitability of spectral indices for evaluating vegetation characteristics on arid rangelands" *Remote Sens. Environ.* 23:213-232.
- Lunetta, R.S., 1998, "Applications, project formulation, and analytical approach," In *Remote Sensing Change Detection: Environmental Monitoring Applications and Methods*, Elvidge, C.D., and Lunetta, R. (Eds.), Ann Arbor Press, MI. pp 1-14.
- Otterman, J., Brakke, T. and J. Smith, 1995, "Effects of leaf transmittance versus leaf-reflectance on bidirectional scattering from canopy/soil surface: an analytical study," *Remote Sens. Environ.* 54: 49-60.
- Roberts, D.A., M.O., Smith, and J.B. Adams, 1993, "Green Vegetation, Nonphotosynthetic Vegetation, and Soils in AVIRIS data," *Remote Sens. Environ.* 44:255-269.
- Smith, M.O., Ustin, S.L., Adams, J.B., and A.R. Gillespie, 1990a, "Vegetation in deserts: I. A regional measure of abundance from multispectral images," *Remote Sens. Environ.* 31, 1-26.
- Smith, M.O., Ustin, S.L., Adams, J.B., and A.R. Gillespie, 1990b, "Vegetation in deserts: II. Environmental influences on regional abundance," *Remote Sens. Environ.* 31, 27-52.
- Ustin, S.L., Smith, M.O., and J.B. Adams, 1993, "Remote Sensing of Ecological Processes: A strategy for developing and testing ecological models using spectral mixture analysis," In *Scaling Physiological Processes: Leaf to Globe*, edited by J.R. Ehleringer and C. Field, (Academic Press Inc.), pp. 339-357.
- Ustin, S.L., D.A. Roberts, and Q.J. Hart, 1998, "Seasonal vegetation patterns in a California coastal savanna derived from Advanced Visible/Infrared Imaging Spectrometer (AVIRIS) data," In *Remote Sensing Change Detection: Environmental Monitoring Applications and Methods*, Elvidge, C.D., and Lunetta, R. (Eds.), Ann Arbor Press, MI. pp. 163-176.
- Yuan, D., C.D. Elvidge, and R.S. Lunetta, 1998, "Survey of multispectral methods for land cover change analysis," In *Remote Sensing Change Detection: Environmental Monitoring Methods and Applications*. R.S. Lunetta and C.D. Elvidge, ed. Ann Arbor Press, MI. pp. 21-35.